Available online at www.sciencedirect.com
ScienceDirect
Journal of Electrical Systems and Information Technology 2 (2015) 197–206
www.elsevier.com/locate/jesit

# Novel SVPWM based on first order equation

Ahmed A. Mansour *

*Electronics Research Institute, Dokki, Cairo, Egypt*

Received 3 May 2015; received in revised form 28 May 2015; accepted 31 May 2015
Available online 12 September 2015

**Abstract**

PWM plays an important role in generating sinusoidal waveform for variable voltage variable frequency drives (VVVFD's) with a minimum harmonic level. PWM techniques have many methods in implementation ranging from a relatively simple method such as modulating sine wave to the advanced Space Vector PWM technique SVPWM. The SVPWM has a dense calculation that requires considerable processor time for execution. The proposed technique requires simple calculations and can be implemented using simple microcontrollers. The calculations of the proposed SVPWM are based on first order equations rather than trigonometric functions requiring either huge lookup tables for fetching or too many instruction cycles for calculation on a digital controller.


*Keywords:* PWM; SVPWM; Space vector modulation; Harmonic elimination

## 1. Introduction

Sinusoidal PWM is the conventional analog technique used in AC motor control. This relatively easy method is implemented by comparing a triangular carrier wave with a sine wave. The points of intersection determine the switching points of the power devices in the inverter. However, this method is unable to make use of the full dc voltage supplying the inverter. Also, the switching characteristics of the PWM produce relatively high harmonic distortion in the inverter's output voltage.

---

*Abbreviations:* $\bar{V}_x$, the generated output vector of the SVPWM; $\bar{V}_A$, component of $\bar{V}_x$ aligned in the directions of the active vectors $\overline{V_1}$; $\bar{V}_B$, component of $\bar{V}_x$ aligned in the directions of the active vectors $\overline{V_2}$; $V_{x\_Max}$, the maximum generated output line vector tangent to the hexagonal; $\overline{V_1}$, the 1st adjacent active vectors to sector 1; $\overline{V_2}$, the 2nd adjacent active vectors to sector 1; $\bar{V}_{0/7}$, the two null vectors; $V_{DC}$, the DC-link voltage of the inverter; $T_S$, sampling frequency of the SVPWM; $T_A$, the applied time of the vector $\bar{V}_A$; $T_B$, the applied time of the vector $\bar{V}_B$; $T_0$, the applied time of the two null vectors; $\frac{T_A}{T_S}$, the per unit of the applied time of the vector $\bar{V}_A$; $\frac{T_B}{T_S}$, the per unit of the applied time of the vector $\bar{V}_B$; $\frac{T_0}{T_S}$, the per unit of the applied time of the null vectors; $m$, the ratio of the line vector of the inverter output to the dc-link voltage; $M$, modulation index; $A_i$, 1st term constants of the 1st order equations for SVPWM; $B_i$, 2nd term constants of the 1st order equations for SVPWM.

* Tel.: +20 1003669801.
*E-mail address:* mansour@eri.sci.eg

Peer review under the responsibility of Electronics Research Institute (ERI).

Production and hosting by Elsevier

http://dx.doi.org/10.1016/j.jesit.2015.05.001

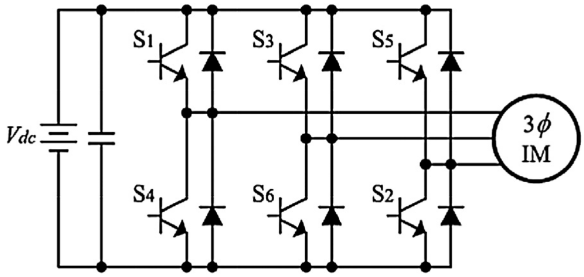


Fig. 1. Three-phase bridge inverter fed induction motor.

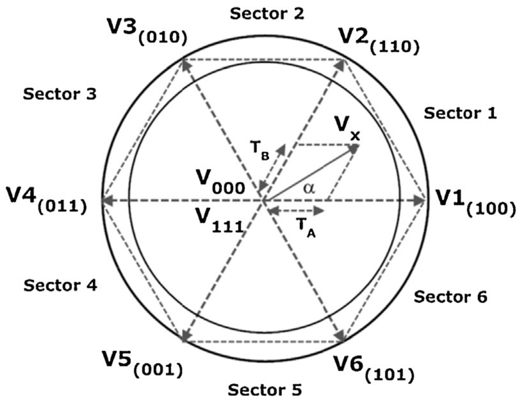


Fig. 2. Space vector hexagon.

Space Vector PWM (SVPWM) is a more sophisticated technique for generating a fundamental sine wave that provides a higher utilization of the dc-link voltage as well as lower total harmonic distortion. It is also compatible for use in vector control (field orientation) of AC motors, also many effort have been done to enhance and to speed up the PWM operation (Alexa and Onea, 2014; Janik et al., 2014; Vasilios and Nikolaos, 2012; Duc-Cuong et al., 2012). Fig. 1 shows the power circuit of 3-phase bridge inverter feeding AC inductive load. The output waveforms of this inverter are based on the switching of the six transistors $T_1, T_2, \ldots, T_6$. The inverter has 8 possible switching states that can be represented as in Fig. 2 of the space hexagon as 6 active vectors ($\overline{V_1}, \overline{V_2}, \ldots, \overline{V_6}$) i.e. (*six voltage steps*) and two null vectors ($V_{000}$, $V_{111}$). Also Table 1 shows the corresponding inverter output of the 8 possible switching states.

If the inverter is switched based only on the six active vectors ($\overline{V_1}, \overline{V_2}, \ldots, \overline{V_6}$) to produce one complete cycle ($2\pi$) as in Fig. 2, so each vector participates a period equal to ($\pi/3$). The output voltage waveforms for both phase voltages

Table 1
Inverter switching states.

| | State | ON devices | $V_{an}$ | $V_{bn}$ | $V_{cn}$ | Space voltage vector |
|---|---|---|---|---|---|---|
| Null | 0 | $T_2\ T_4\ T_5$ | 0 | 0 | 0 | $V_0$ (0 0 0) |
| | 1 | $T_1\ T_4\ T_6$ | 2/3 $V_{dc}$ | −1/3 $V_{dc}$ | −1/3 $V_{dc}$ | $V_1$ (1 0 0) |
| | 2 | $T_1\ T_3\ T_6$ | 1/3 $V_{dc}$ | 1/3 $V_{dc}$ | −2/3 $V_{dc}$ | $V_2$ (1 1 0) |
| Six voltage steps | 3 | $T_2\ T_3\ T_6$ | −1/3 $V_{dc}$ | 2/3 $V_{dc}$ | −1/3 $V_{dc}$ | $V_3$ (0 1 0) |
| | 4 | $T_2\ T_3\ T_5$ | −2/3 $V_{dc}$ | 1/3 $V_{dc}$ | 1/3 $V_{dc}$ | $V_4$ (0 1 1) |
| | 5 | $T_2\ T_4\ T_5$ | −1/3 $V_{dc}$ | −1/3 $V_{dc}$ | 2/3 $V_{dc}$ | $V_5$ (0 0 1) |
| | 6 | $T_1\ T_4\ T_5$ | 1/3 $V_{dc}$ | −2/3 $V_{dc}$ | 1/3 $V_{dc}$ | $V_6$ (1 0 1) |
| Null | 7 | $T_1\ T_3\ T_5$ | 0 | 0 | 0 | $V_7$ (1 1 1) |

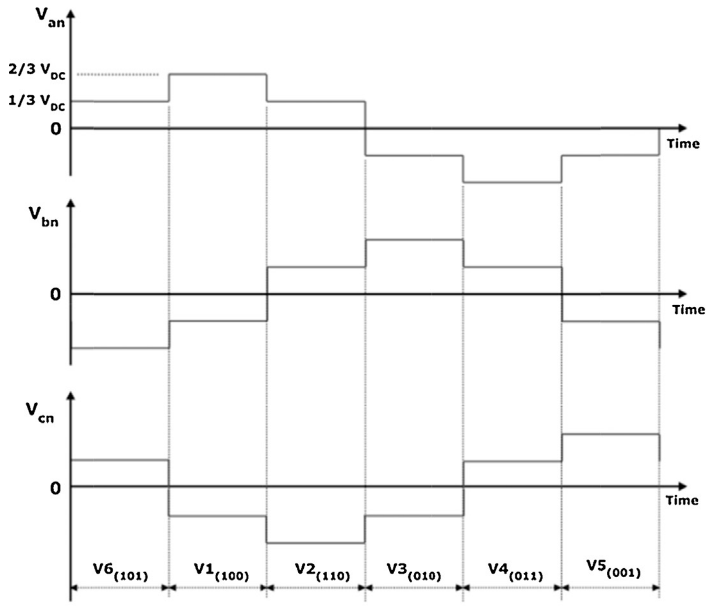


**(a)** Phase voltages

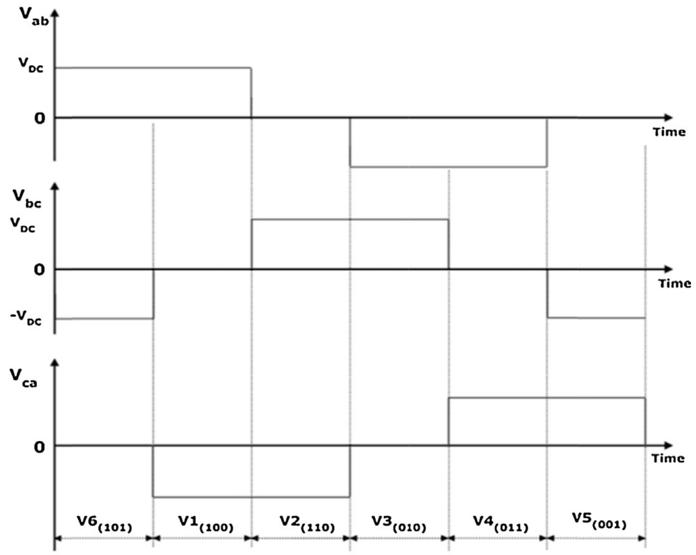


**(b)** Line voltages

Fig. 3. Out-put voltages of six step inverter.

and line voltages are shown in Fig. 3. It is clear that the max.(peak) of the phase voltage is ($V_{an} = (2/3)V_{DC}$) and the corresponding peak line voltage is $V_{DC}$. This output has a large harmonic distortion.

To generate sinusoidal waveform at the output of the inverter, we must generate a switching pattern that produces a voltage at not only the six vectors states but also one at each transition in between these states. So the SVPWM is based on both the six active vectors and the two null vectors to produce a rotating vector with a fixed magnitude at the inner hexagonal shown in Fig. 2.

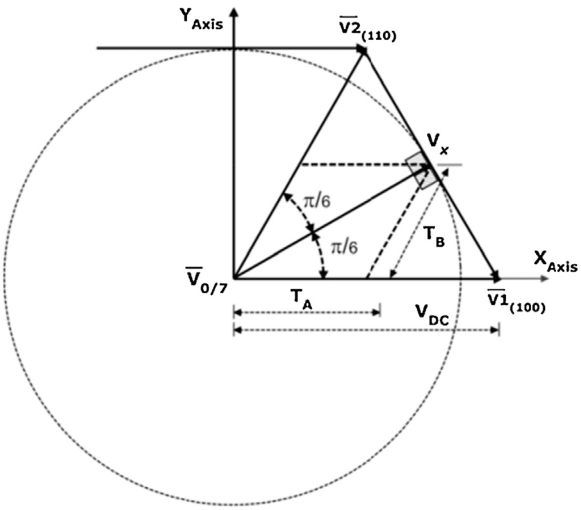


Fig. 4. Max. generated line vector $\bar{V}_{x\_Max}$ from the hexagonal.

## 2. Mathematical equations

For SVPWM, it seeks to average out the adjacent active vectors for each sector. Consider sector 1 as shown in Fig. 4, bounded by Vectors 1 0 0, 1 1 0 and the two null vectors $\bar{V}_0$ (0 0 0) and $\bar{V}_7$ (1 1 1). So the maximum peak of the line voltage can be generated from the SVPWM at the inverter output is described in Eq. (1). This maximum peak $\bar{V}_{x\_Max}$ is achieved when the locus of the vector $\bar{V}_x$ make a circle tangent to the inner of the hexagon shown in Fig. 4.

The ratio of the line vector of the inverter output to the dc-link voltage $m = |V_x| / V_{DC}$, so the maximum generated line voltage is as in Eq. (1).

$$V_{x\_Max} = V_{DC} \times \frac{\sqrt{3}}{2} \tag{1}$$

So the inverter output line voltage is controlled via controlling the ratio of the line output voltage to dc link voltage from ($m = 0$ to $m_{\max.} = \sqrt{3}/2$).

As shown in Fig. 5, the vector $\bar{V}_x$ with angle ($\alpha$) is the resultant of the vector addition of both $\bar{V}_A$ and $\bar{V}_B$ as in Eq. (2).

$$\bar{V}_x = \bar{V}_A + \bar{V}_B \tag{2}$$

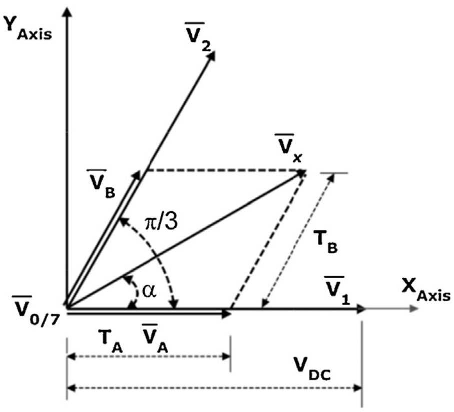


Fig. 5. Vector $\bar{V}_x$ in sector 1.

where $\bar{V}_A$ and $\bar{V}_B$ are the components of $\bar{V}_x$ aligned in the directions of the two active vectors $\bar{V}_1$ and $\bar{V}_2$ (i.e. $V1\,0\,0$ and $V1\,1\,0$) respectively. $\bar{V}_x$ can be approximated by applying $V1\,0\,0$ for a percentage of time $T_A$.and $V1\,1\,0$ for a percentage of time $T_B$ over a period $T_s$.

The average volt seconds along the $X$–$Y$ axis produced by the vectors $\bar{V}_1$, $\bar{V}_2$ and $\bar{V}_{0/7}$ is equal to the volt seconds of the vector $\bar{V}_x$ over a switching period $T_s$ as in Eq. (3).

$$\bar{V}_x \times T_s = (T_A \times \bar{V}_1) + (T_B \times \bar{V}_2) + (T_0 \times \bar{V}_{0/7}) \tag{3}$$

So,

$$\bar{V}_x = \left(\frac{T_A}{T_s}\bar{V}_1\right) + \left(\frac{T_B}{T_s}\bar{V}_2\right) + \left(\frac{T_0}{T_s}\bar{V}_{0/7}\right) \tag{4}$$

Resolving $\bar{V}_x$ vector along both $X$ and $Y$ axes Eqs. (5) and (6) are presented as follows:

$$\left|\bar{V}_x\right| \cos(\alpha) \times T_s = V_{DC} \times T_A + V_{DC} \times \cos\left(\frac{\pi}{3}\right) \times T_B \tag{5}$$

$$\left|\bar{V}_x\right| \sin(\alpha) \times T_s = V_{DC} \times \sin\left(\frac{\pi}{3}\right) \times T_B \tag{6}$$

So, from Eqs. (1), (3)–(6) the two per unit times $T_A/T_s$, and $T_B/T_s$ of both active vectors $\bar{V}_A$ and $\bar{V}_B$ are expressed as in Eqs. (7) and (8).

$$\frac{T_A}{T_s} = \frac{2}{\sqrt{3}} \times m|_0^{\frac{\sqrt{3}}{2}} \times \sin\left(\frac{\pi}{3} - \alpha\right) \tag{7}$$

$$\frac{T_B}{T_s} = \frac{2}{\sqrt{3}} \times m|_0^{\frac{\sqrt{3}}{2}} \times \sin(\alpha) \tag{8}$$

So, Eqs. (7) and (8) can be reduced in the next forms:

$$\frac{T_A}{T_s} = M \times \sin\left(\frac{\pi}{3} - \alpha\right) \tag{9}$$

$$\frac{T_B}{T_s} = M \times \sin(\alpha) \tag{10}$$

where $M = 2/\sqrt{3} \times m|_0^{\frac{\sqrt{3}}{2}}$ is the modulation index.

This modulation index varies from $(M = 0\,\text{at}\,m|_{=0})$ to $\left(M = 1 \quad \text{at}\,m_{\max}|_{=\frac{\sqrt{3}}{2}}\right)$.

So, a controllable line vector of amplitude range varies from $0 \le V_x \le V_{x\_Max}$ is produced based on modulation index "$M$" where $0 \le M \le 1$.

The SVPWM switching time as in Eq. (11) is the sum of the applied time to the two active vectors (i.e. $\bar{V}_1$ and $\bar{V}_2$) and the time applied to both null vectors $\bar{V}_{000}$ and $\bar{V}_{111}$.

$$T_S = T_A + T_B + T_{0/7} \tag{11}$$

So, the null vector time $T_0$ is expressed as in Eq. (12)

$$T_0 = T_s - T_A - T_B \tag{12}$$

And, the per unit time of the null vector $T_0$ is expressed as in Eq. (13)

$$\frac{T_0}{T_s} = 1 - \frac{T_A}{T_s} - \frac{T_B}{T_s} \tag{13}$$

The last equations can be applied for all sectors from 1 to 6 taking into consideration only the switching pattern of each sector.

Fig. 6 shows the variation of the per unit times $T_A/T_s$, $T_B/T_s$, and $T_0/T_s$ of both active vectors and the null vectors against angle ($\alpha$) from (0° to 60°) at different modulation indices $M = 1$, $M = 0.5$, and $M = 0.1$ respectively. It is clear that the per unit times $T_A/T_s$, $T_B/T_s$ of the two active vectors are directly proportional to the modulation index. As well

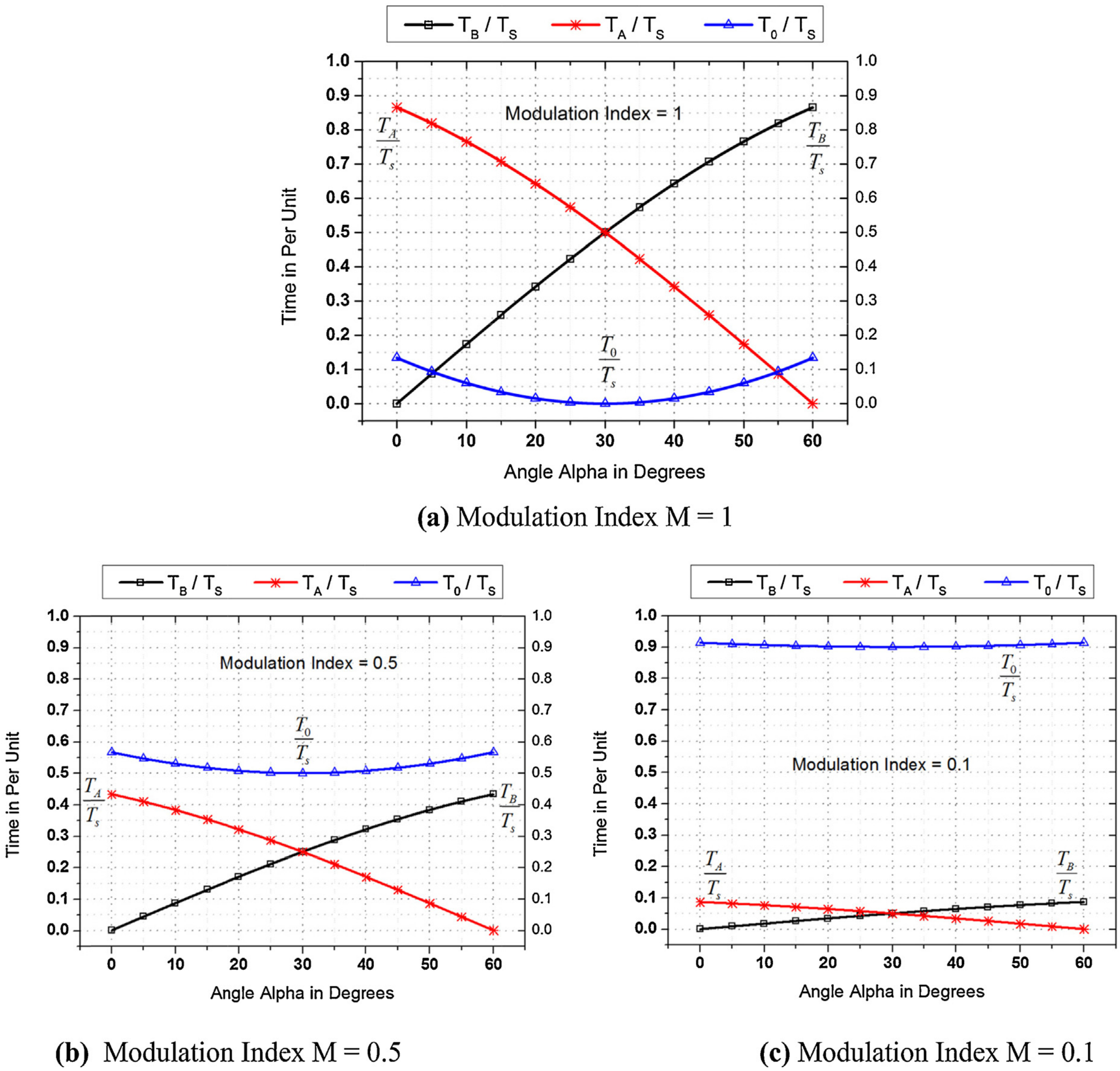


**(a)** Modulation Index M = 1

**(b)** Modulation Index M = 0.5

**(c)** Modulation Index M = 0.1

Fig. 6. The per unit $T_A$, $T_B$, $T_0$ versus the vector position angle Alpha @ different modulation index.

as the per unit time of the $T_0/T_s$ is inversely proportional to the modulation index. This means that to get large output voltage at the inverter terminals the two active vectors have time sharing greater than that of the corresponding time of the two null vectors, and vice versa.

Figs. 7–9 show the effect of changing the modulation index on the per unit of $T_A$, $T_B$ and $T_0$ individually versus the vector position angle Alpha respectively.

## 3. Problems and idea of the proposed SVPWM

### 3.1. Problems of SVPWM

From the last Eqs. (9) and (10), it is clear that the SVPWM time calculations are based on trigonometric function. For real time applications based on both microcontroller and DSP techniques, the SVPWM technique consumes much time for calculating these functions or lookup tables should be provided with sufficient resolution to fetch them which

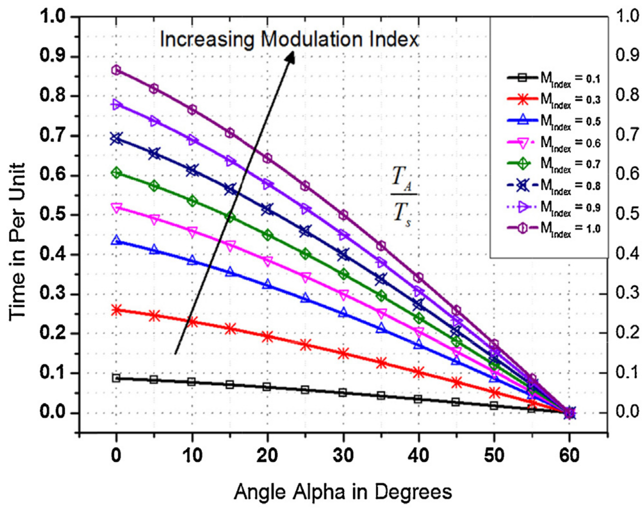


Fig. 7. The per unit of $T_A$, versus the vector position angle Alpha.

requires large storage space for V/F control algorithms. Although a lookup table of the sine or cosine function is stored to overcome the online time calculations of these functions, where many instruction cycles are consumed to calculate the trigonometric functions, also it needs further calculations for interpolation and requires large storage space.

Also, for V/F applications, the SVPWM has some problems at low frequencies. For example the SVPWM operates with switching frequency 10KHz, at low frequencies starting from 1 Hz, SVPWM needs 10,000 vector positions along the 6 sectors to get one complete cycle of the sine wave at fundamental frequency 1 Hz (i.e. 1666.66 vector positions) and each position has three locations for pre calculated times of $T_A$, $T_B$, and $T_0$. This means a lookup table of length equal to three times the total vector position (i.e. $3 \times 1666.66 = 5000$). So, to generate 1 Hz sine wave, a lookup table of 5000 locations/sector is needed. So, the previous problem needs sophisticated microcontrollers having both high memory capacity and high speed to overcome the execution time of the trigonometric function, where the SVPWM represents the core of the control algorithm in the variable speed drives.

Then, what is the solution? The proposed technique is simpler and more convenient for implementing the SVPWM faster and cheaper by using unsophisticated microcontroller system.

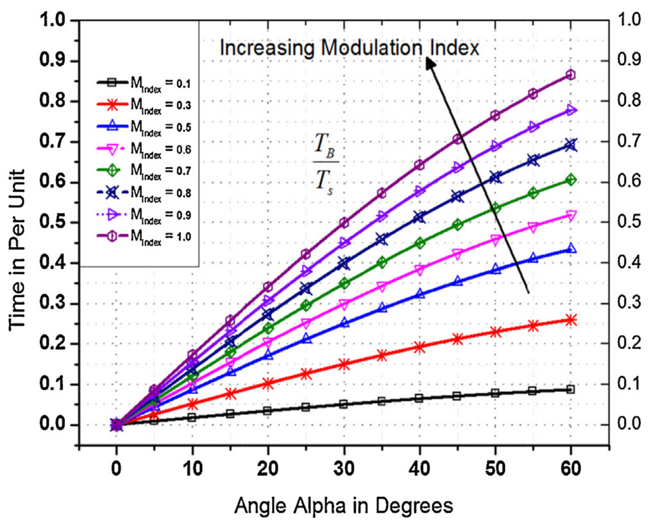


Fig. 8. The per unit of $T_B$, versus the vector position angle Alpha.

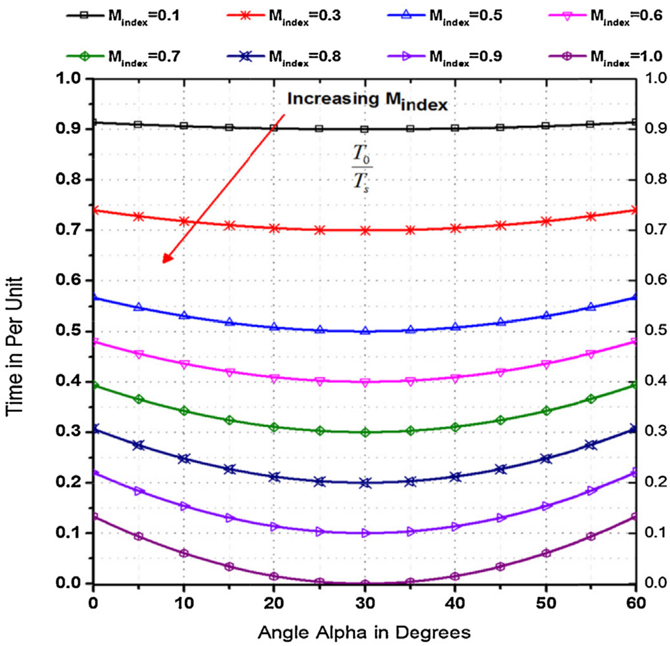


Fig. 9. The per unit of $T_0$ versus the vector position angle Alpha.

### 3.2. Proposed SVPWM

It is clear from Fig. 6 that the time of the two active vectors $T_A$ and $T_B$ are mirrored (i.e. $T_A$ equation at angle $\alpha = 0°$ gives the same value calculated from $T_B$ equation at angle $\alpha = 60°$). So at any vector position at angle $\alpha°$ one equation can be used to calculate both $T_B$, and $T_A$ at angle $\alpha$ and angle $(60 - \alpha)$ as shown from Eqs. (9) and (10) respectively.

The idea of the proposed technique is based on curve fitting of a segmented curve shown in Fig. 10. To get more accurate calculations for $T_A$, $T_B$, and $T_0$ each segment should be as small as possible. This curve is divided into 24 segments that cover the full range of the vector positions from ($\alpha = 0°$ to $\alpha = 60°$). So each segment covers 2.5° individually.

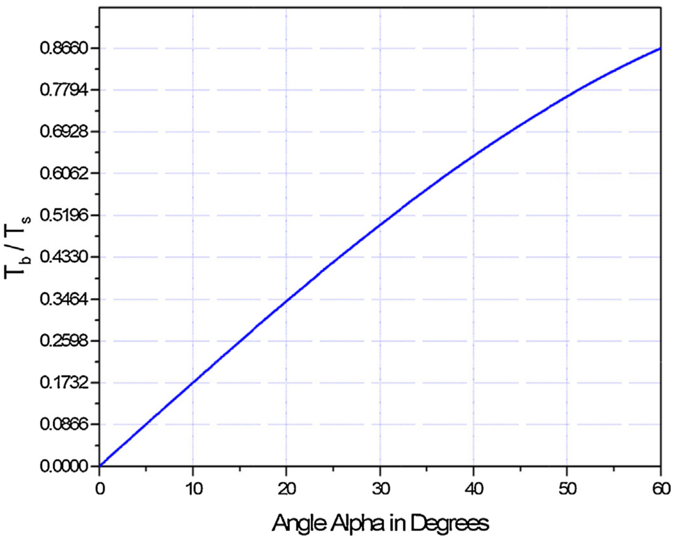


Fig. 10. $T_b$ versus the vector position angle Alpha.

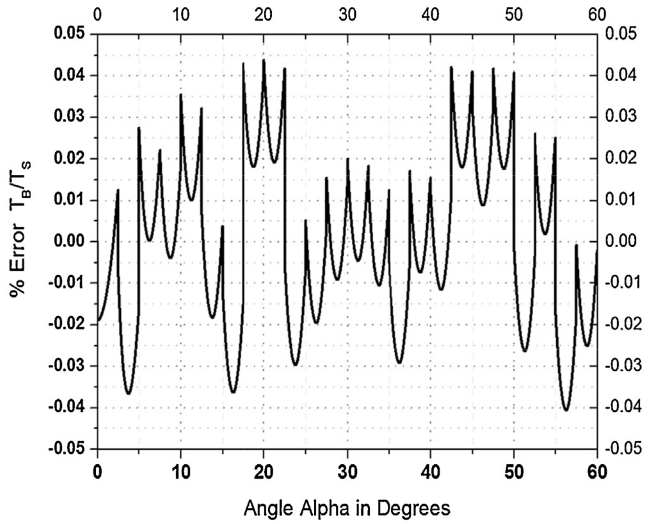


Fig. 11. The percentage error % $T_{b\text{-}error}$ versus the vector position angle ($\alpha$).

This approach leads to getting 24 sectors to make the curve as close as possible to straight line. These sectors produce a 24 first order equations that are simpler in calculations than that based on trigonometric sine functions. So the SVPWM is based on the first order equations.

The total numbers of equations are equal to 24 as shown in Eqs. (14) and (15) which are simpler than that in Eqs. (11) and (12) of trigonometric function.

$$\left(\frac{T_B}{T_s}\right)_{i=(1-24)} = M \times (A_i + B_i \times \alpha^\circ) \tag{14}$$

$$\left(\frac{T_A}{T_s}\right)_{i=(1-24)} = M \times (A_{(25-i)} + B_{(25-i)} \times (60^\circ - \alpha^\circ)) \tag{15}$$

See Appendix A for 24 segment equations' constants $A$'s and $B$'s.

Now the SVPWM has no need for sophisticated microcontrollers, it is simpler and faster in implementation. The only problem appearing here is the code length that has 24 first order equations written in "C" code based on switch(i) function command which get the index no. based on the range of vector position angle ($\alpha$), (i.e. $i = 1$ for ($0^\circ \le \alpha < 2.5^\circ$), $i = 2$ for ($2.5^\circ \le \alpha < 5^\circ$), . . ., $i = 24$ for ($57.5^\circ \le \alpha < 60^\circ$)).

So, based on the index which defines the range, only one equation is used for computing the SVPWM times $T_A$, $T_B$, and $T_0$.

Also, the Fig. 11 shows the percentage of error of the $T_B$, between calculations by trigonometric equation and the fitted equations calculations refer to Eqs. (12) and (14). It is clear that percentage error between the calculations of the two equations is around (0.045% to −0.045%) along the angle ($\alpha$) which is very trivial error.

## 4. Conclusions

This paper introduced a new SVPWM technique based on first order equation. This technique is easier, faster, and simpler than the conventional SVPWM technique, which is based on trigonometric functions which suffers from complexity, and consuming large time in implementation. Also, our proposed technique have a minimal error which reaches the range (0.05% to −0.05%). This error is very small compared to the simplicity of calculations.

## Acknowledgment

The author is grateful to the Electronics Research Institute, Dokki, Cairo, Egypt for subsiding this research.

## Appendix A.

See Table A1.

Table A1
Parameters of the first order equations for calculating $T_A/T_s$, and $T_B/T_s$ for SVPWM.

| Equation no. | $A_i$ | $B_i$ | Range of angle ($\alpha$) |
|---|---|---|---|
| 1 | 0 | 0.01745 | $(0.0° \le \alpha < 2.50°)$ |
| 2 | 9.17E−05 | 0.01741 | $(2.5° \le \alpha < 5.00°)$ |
| 3 | 4.30E−04 | 0.01735 | $(5.0° \le \alpha < 7.50°)$ |
| 4 | 0.00118 | 0.01725 | $(7.5° \le \alpha < 10.0°)$ |
| 5 | 0.00251 | 0.01712 | $(10.0° \le \alpha < 12.5°)$ |
| 6 | 0.00458 | 0.01695 | $(12.5° \le \alpha < 15.0°)$ |
| 7 | 0.00754 | 0.01675 | $(15.0° \le \alpha < 17.5°)$ |
| 8 | 0.01156 | 0.01653 | $(17.5° \le \alpha < 20.0°)$ |
| 9 | 0.01677 | 0.01627 | $(20.0° \le \alpha < 22.5°)$ |
| 10 | 0.02334 | 0.01597 | $(22.5° \le \alpha < 25.0°)$ |
| 11 | 0.03139 | 0.01565 | $(25.0° \le \alpha < 27.5°)$ |
| 12 | 0.04107 | 0.0153 | $(27.5° \le \alpha < 30.0°)$ |
| 13 | 0.0525 | 0.01492 | $(30.0° \le \alpha < 32.5°)$ |
| 14 | 0.0658 | 0.01451 | $(32.5° \le \alpha < 35.0°)$ |
| 15 | 0.0811 | 0.01407 | $(35.0° \le \alpha < 37.5°)$ |
| 16 | 0.09849 | 0.01361 | $(37.5° \le \alpha < 40.0°)$ |
| 17 | 0.11807 | 0.01312 | $(40.0° \le \alpha < 42.5°)$ |
| 18 | 0.13995 | 0.01261 | $(42.5° \le \alpha < 45.0°)$ |
| 19 | 0.16419 | 0.01207 | $(45.0° \le \alpha < 47.5°)$ |
| 20 | 0.19086 | 0.01151 | $(47.5° \le \alpha < 50.0°)$ |
| 21 | 0.22003 | 0.01092 | $(50.0° \le \alpha < 52.5°)$ |
| 22 | 0.25176 | 0.01032 | $(52.5° \le \alpha < 55.0°)$ |
| 23 | 0.28607 | 0.00969 | $(55.0° \le \alpha < 57.5°)$ |
| 24 | 0.32301 | 0.00905 | $(57.5° \le \alpha < 60.0°)$ |

## References

Alexa, I.-A., Onea, A., 2014. Fast calculating PWM techniques of voltage source inverter. In: Proceedings of the 18th International Conference on System Theory, Control and Computing, Sinaia, Romania, October 17–19, pp. 526–531.

Janik, D., Kosan, T., Sadsky, J., Peroutka, Z., 2014. Implementation of SVPWM algorithm without trigonometric functions. In: Proceedings of 19th International Conference on Applied Electronics, Pilsen, 9–10 September, pp. 131–134.

Vasilios, I.C., Nikolaos, M.I., 2012. A Novel SVPWM overmodulation technique based on voltage correcting function. In: 3rd IEEE International Symposium on Power Electronics for Distributed Generation Systems (PEDG), pp. 682–689.

Quach, D.-C., Yin, Q., Shi, Y.-F., Zhou, C.-J., 2012. Design and implementation of three-phase SVPWM inverter with 16-bit dsPIC. In: 12th International Conference on Control, Automation, Robotics & Vision, Guangzhou, China, 5–7th December (ICARCV 2012), pp. 1181–1186.